

# Comprehensive Evaluation in Real Slab Reheating Furnace with Highly Preheated Air Combustion

Masao Uede

R&D div. Chugairo co., ltd.  
Masao\_Uede@n.chugai.co.jp

Toshio Shimada

R&D div. Chugairo co., ltd.  
Toshio\_Shimada@n.chugai.co.jp

Noriyuki Tokudome

Plant div. Chugairo co., ltd.  
Noriyuki\_Tokudome@n.chugai.co.jp

Morihiko Imada

R&D div. Chugairo co., ltd.  
Morihiko\_Imada@n.chugai.co.jp

*Keywords: Reheating Furnace, Highly Preheated Air Combustion,  $\phi_{cg}$ ,  $NO_x$ , Skid Mark,*

## ABSTRACT

Highly preheated air combustion technology has been applied to a large number of industrial furnaces, and consequently energy saving along with the reduction of  $NO_x$  emission have been achieved. The technology contains regenerative burners used in slab reheating furnaces. The following items were clarified as a result of an evaluation based on operation data obtained from the furnace.

- 1) The coefficient of overall heat transfer ( $\phi_{cg}$ ) calculated from the actually measured temperature in the furnace was 0.95. This is approximately 20% higher than conventional furnaces.
- 2) The temperature deviation after rough rolling was 10°C. Compared with conventional furnaces, there has been a 30% improvement.
- 3) The quantity of  $NO_x$  emission was reduced by one-third compared with conventional furnaces.
- 4) The delivery was completed in nine months after the design start, and has been conventionally shortened by nine months.

## INTRODUCTION

The high performance industrial furnace project, carried out by NEDO and JIFMA, was from 1993 to 2002. The targets of the project were energy saving by 20%, downsizing by 30% and reduction of  $NO_x$  by 50%. The key technology to the project was the highly preheated air combustion method, which needs a regenerative technique. Using pilot plants, tests in various shapes of furnaces were made before a practical application. [1][2][3] The results of the tests were favorable as follows;

- 1) An Expanded flame made temperature distribution flat.
- 2) A Low  $NO_x$  was achieved by low oxygen concentration combustion.
- 3) The Heat-conducting efficiency was improved.
- 4) Fuel was ignited at a higher temperature than self-ignition.

However, as those tests were carried out by pilot plants instead of in an operating furnace, the evaluation was not suppose to be fair. This is to report the analysis based on real data and CFD of the results of the highly preheated air combustion method in commercially operating furnaces.

On the other hand, our customer requested us to shorten the delivery period to 9 months, since they thought a shortened period, would enable them to react to the steep change of economic situations and to get an advantageous cash flow. The cooperation among design,

manufacturing and construction fulfilled their requirements by shortening the delivery period.  
Our efforts are shown as follows;

## 1. Reheating Furnace Evaluation

This evaluated furnace (NKK Fukuyama Works), which was done as a basic design in collaboration with NKK Corporation who has a lot of experience in regenerative burner heating systems adopted the regenerative burner to all zones and had the burners arranged on the side walls. Fig.1 shows a longitudinal section view. The regenerative burners are indicated by 19 circles on both upper and lower sides. The standard specifications are shown as follows;

Dimensions	36(l)*10.1(w)*4.8(h)m
Heating Capacity	200 ton/h Max.230 ton/h
Fuel	Mix-Gas
Low Calorific Value	11.7MJ/m <sup>3</sup> N
Material	Mild Steel
Slab size	8.8(l) *1.5(w)* 0.22(t)
Slab weight	21800kg
Treatment Temperature	20→1250°C
Burner Capacity	1100 to 3500kW total 76 Burners
Control Zone	4 zones 10 sections

Fig. 2 shows a schematic drawing for regenerative burner, which was developed by NKK Corporation and NFK Ltd.

The preheated air inlet is arranged on the burner axis; and the fuel inlets that are at an angle to the horizontal are arranged around it. This burner has two firing modes. When the furnace temperature is under 800°C, the fuel is led into the furnace from the air inlet. The main flame is kept by the pilot burner. When the furnace temperature is over 800°C, the fuel is led into the furnace from the two fuel inlets.

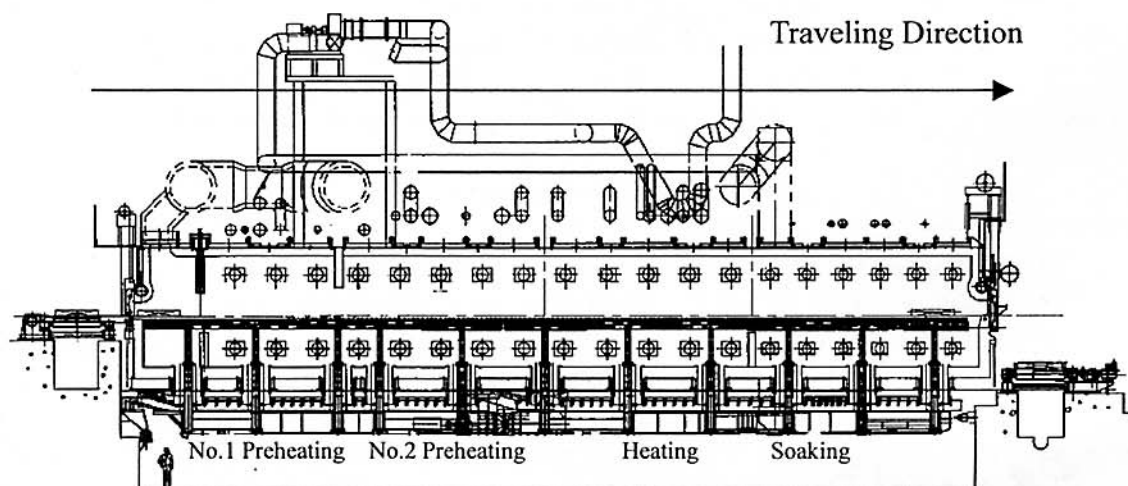


Fig.1 Reheating Furnace

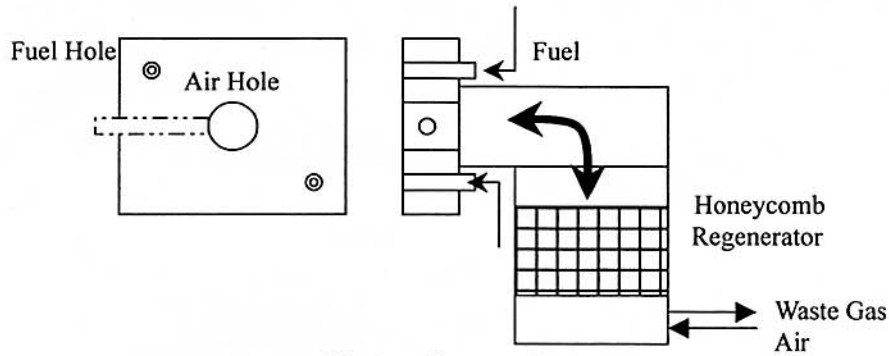


Fig.2 Shape of Burner

## 2. CFD

Thermal fluid analyzing code STAR-CD which adopted the finite volume method. For turbulent fluid field calculations, it adopts  $k-\varepsilon$  method [4], and for combustion calculation it adopts the PDF (probability density function) model [5]. The radiation from the wall and gas were taken into account with DTRM model[6].

## 3. Results

### 3.1 Furnace temperature distribution

One of the important requirement for the reheating furnace is the uniformity of the temperature distribution. Especially the temperature slope in the furnace width is directly related to the material temperature distribution.

Fig.3 shows the measurement and the calculation result of the temperature distribution at the ceiling surface. The furnace width is shown as the x axis. The shapes of the measured temperature profiles appears flat or a slightly convex form. Since the material temperature of No.1 preheating zone is low, temperature distribution tends to show a concave tendency. However, it appears slightly convex in No.2 preheating zone and is of a suitable distribution profile for heating slab. Although the temperature deviation was  $\pm 23^\circ\text{C}$ , highest at No.2 preheating zone, it can be thought of as a flat temperature distribution. We assumed  $500^\circ\text{C}$  is the typical to calculate. The temperature is equal to the point between No.1 and No.2 preheating zones. The average temperature of two zones is the modified temperature. This temperature profile has the same tendency for the measured profile.

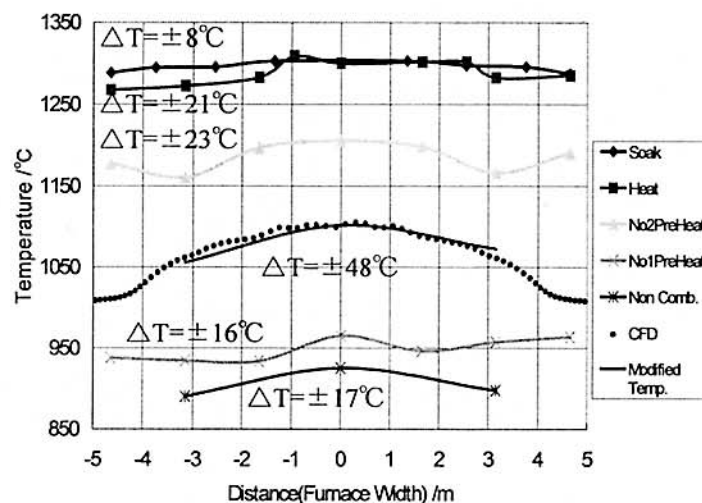


Fig.3 Temperature distribution as a function of Furnace width

The dotted line shows the CFD's ceiling temperature at the modified point. The calculated value shows of a deviation of  $\pm 48^\circ\text{C}$ . The error of the calculated value is due to the boundary condition of the material surface temperature which was set at  $500^\circ\text{C}$  rigidly.

### 3.2 Characteristic of heat-conducting and estimated overall heat transfer coefficient ( $\phi_{cg}$ )

In order to make a clear characteristic for highly preheated air combustion we calculated the overall heat transfer coefficient( $\phi_{cg}$ ) by heat conduction analysis with measured furnace temperature and slab temperature. Fig.4 shows furnace, slab (measured, simulated) temperature distribution and estimated  $\phi_{cg}$  as a function of time history. This furnace temperature is the ceiling temperature above and moving with the slab. It is shown that the furnace temperature rises rapidly by the effects of the partition wall. The  $\phi_{cg}$  is a decided 0.95 by parameter fitting when the simulated temperature trace is the closest to the experimental result. This result is considered to be  $\phi_{cg}$  in the furnace which used the highly preheated air combustion method, and the same arrange burner is in agreement.

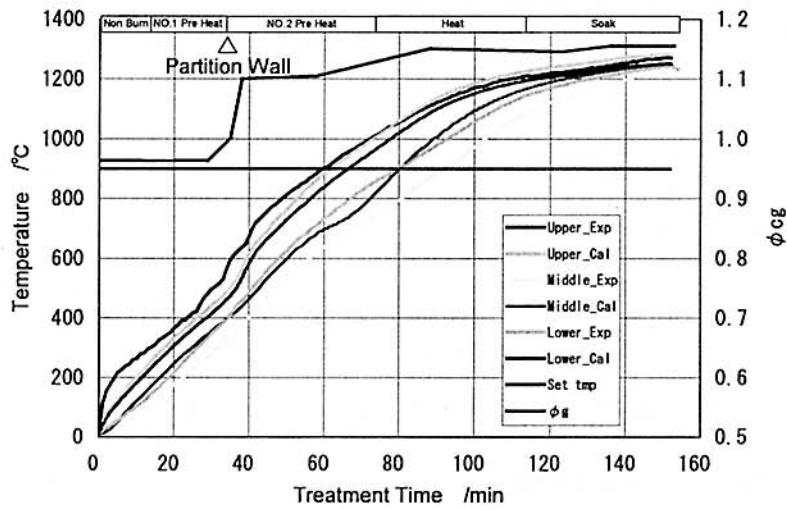


Fig.4 Furnace, Slab (Measured, Simulated) Temperature distribution and Estimated  $\phi_{cg}$  as a function of Time history

The estimated overall heat transfer coefficient( $\phi_{cg}$ ) of the highly preheated air combustion method is improved about 20% compared with the conventional one. It can be assumed that  $\phi_{cg}$  is higher because the deviation of the temperature of this furnace is small. The cause of the reduction of a temperature deviation is discussed below. The injection velocities of fuel and air for the regenerative burner are large in order to improve the mixture of fuel, preheated air and exhaust gas in a furnace. Fig.5 shows air velocity attenuations by CFD as a function of non-dimensional distance, which is described in Eq.(1).

$$Y=X/A \quad \text{---(1)} \quad X_c=(C-(A+B)/2)/2\tan \theta \quad \text{---(2)}$$

Y: Non-dimensional Distance X: Distance from burner Xc: Cross point

A: Diameter for air inlet B: Diameter for gas inlet C: Nozzle pitch

$\theta$  : Expansion half angle

The non-dimensional distance 7 in the potential core region is almost the same. However, in the case of the high speed flow in the entrainment region, we find the velocity attenuation is increased. The attenuation of velocity from burner to distance 10 is large compared to other portions. This is because of the large turbulent energy. If the expansion angles of both the air and the fuel jets are the same rigid degrees[7], Xc is shown in Eq.(2). The Xc point is

shown as the imaginary jets of air and gas cross point in Fig.6.

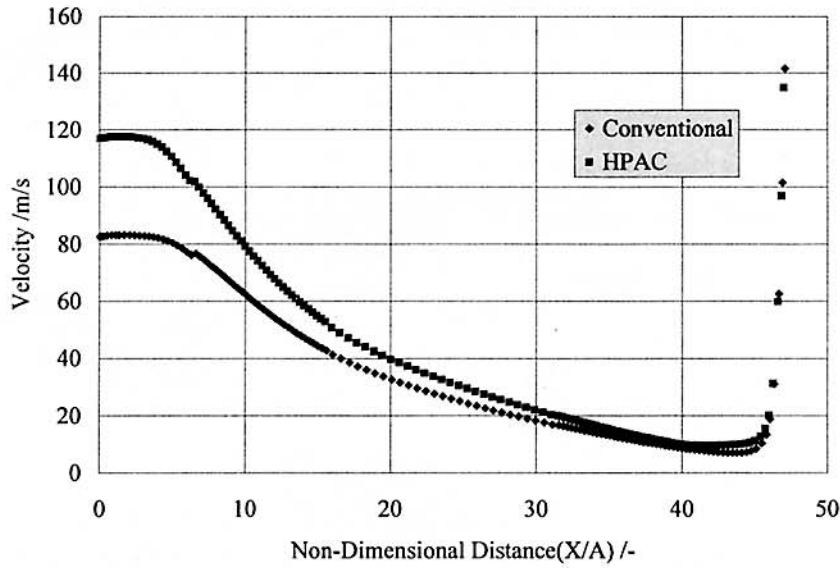


Fig.5 Air Velocity distribution at temperature vs. Non-dimensional distance

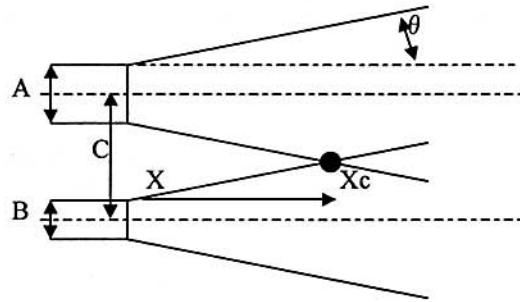


Fig.6 Cross point for two jets

If the combustion starts at this  $X_c$ , a starting point of non-dimensional distance of the burner shown in Fig.2 is 10.6. These phenomena allow us to predict that the combustion starts in an atmosphere, which is mixed with flue gas, preheated air and fuel, that has a low oxygen and/or low fuel concentration.

The well mixing of gas species is done from a geometric point of view. Two fuel holes are on the opposite corner of the burner tile in order to separate them from the air hole. It is required for the long distance to meet the fuel and the air jet. Therefore, the combustion in the low concentration of oxygen at the start of combustion is possible. Fig.7 shows an analysis of the temperature distribution at the height of the preheated air inlet and fuel inlet. In this figure, an area of high temperature is small.

These results, which are considered as the evidence of a start of combustion in low oxygen or low fuel concentration, make a combustion in a distant region from the burners and expand the flame area and make the deviation of the temperature small. In addition, it also may be a factor that this is the most suitable furnace size[8] that is researched in the Development of High performance Industrial Furnace PJ.



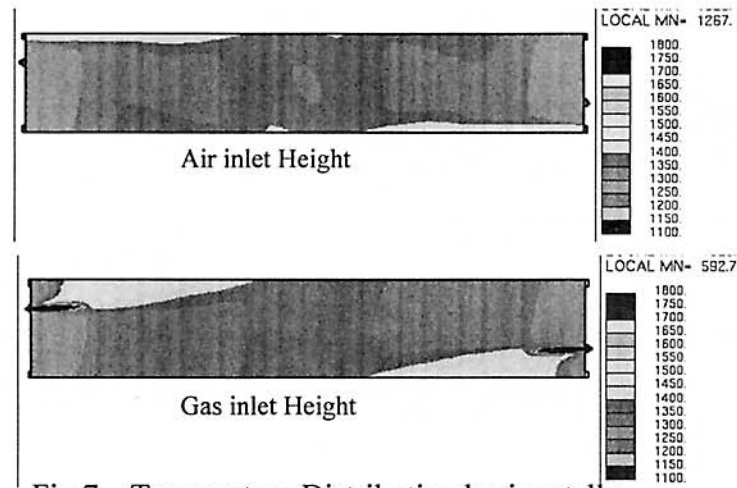


Fig.7 Temperature Distribution horizontally

### 3.3 Reduction of skid marks

Fig.8 is abstracted data from a pen-recorded chart of the slab surface temperature after rough rolling. Skid mark value is  $10^{\circ}\text{C}$  and has improved 30% at  $15^{\circ}\text{C}$  in the conventional furnace. The temperature deviation at the end time of heating is presumed to be about  $15\text{--}20^{\circ}\text{C}$ . We can find that the slab temperature is low at an anti-mill side. It is considered to be due to the imbalance of combustion control occurring in the soaking zone. The combustion control is not adequate because the control zone is divided with the slabs that are brought near by the mill side.

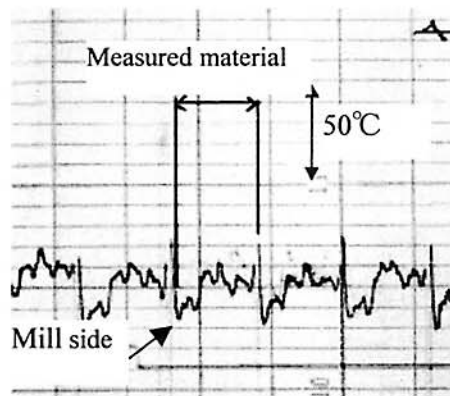


Fig.8 Slab Temperature distribution after rough rolling from pen-recorded chart



Fig.9 Flame Distribution around the Walking Post in Lower Zone

Fig. 9 shows the insight of the reheating furnace from the sight hole. The left photograph shows the inner portion during exhausting. The right shows the same during combusting.

In combusting, the post of WB is bright and is surrounded with the thin flame. The post surface temperature was  $1600^{\circ}\text{C}$  measured by a thermocouple. The temperature of the post was under  $1600^{\circ}\text{C}$ .

This part is made of a  $1600^{\circ}\text{C}$ -resistant refractory and adequate fire resistance was observed during the test period. It is supposed that the material is heated up by the radiation from the post surface under  $1600^{\circ}\text{C}$ .

The current density, when the flame impinged the post, was measured in another test. The density of the regenerative burner is higher than that of the conventional burner. The ionizing flame achieves a flat temperature distribution, as the cooled-down flame by ionization was heated up again by deionization. In other words, the whole flame energy is preserved as ionizing energy is deionizing and returns to heat energy before reheating materials, while the flame is robbed of the heat energy in ionizing.

The direct radiation from the flame makes the shade of constructions inside the furnace, causing the uneven heating. On the other hand, in indirect radiation, after the heat of the flame is absorbed by the constructions and/or wall, it is conveyed fully to the materials. Therefore, indirect radiation makes little shade, can heat materials evenly and makes skid marks negligible.

### 3.4 $\text{NO}_x$ Reduction

Fig. 10 shows the change of the  $\text{NO}_x$  concentration in a chimney and an exhaust pipe after heat recovery. The time average of  $\text{NO}_x$  level converted into 11% oxygen concentration is 20 ppm, one-third of conventional furnaces.

Generally,  $\text{NO}_x$  within a chimney consists of thermal  $\text{NO}_x$  and fuel  $\text{NO}_x$ . Thermal  $\text{NO}_x$  comes into existence as a result of the reaction between nitrogen in the air and firing oxygen, though fuel  $\text{NO}_x$  results from the reaction between nitrogen in the fuel and firing oxygen. In the reheating furnace, particularly, thermal  $\text{NO}_x$  occupies most of exhaust  $\text{NO}_x$ .

In order to regulate the thermal  $\text{NO}_x$  emission in Highly Preheated Air Combustion, it is important to reduce the high temperature combusting area. For that purpose, the ionizing enables the reduction of the combustion temperature.

The analysis of the atmosphere sampled from the furnace ceiling shows a carbon monoxide concentration over 6000 ppm. Considering that the CO in the furnace is an intermediate, this fact indicates the reaction is in progress and the atmosphere temperature is cooled down in the center of the furnace.

As mentioned in 3.2, preheated air and fuel which are injected at high speed entrain the exhaust gas and are mixed with the atmosphere in the furnace. The heat energy is used to heat up the temperature of the exhaust gas such as  $\text{N}_2$ ,  $\text{H}_2\text{O}$  and/or  $\text{CO}_2$ .

Since the preheated air and fuel is diluted by exhaust gas, the combustion occurs in a lower  $\text{O}_2$  concentration. The local high temperature area disappears, thanks to the above reason.

Sarofin says less thermal  $\text{NO}_x$  is generated under  $1550^{\circ}\text{C}$  [10]. We should control the combustion temperature under it.

The result of CFD is shown in Fig. 7. The temperature near the burner was under  $1550^{\circ}\text{C}$ . The above theories lead to a lower thermal  $\text{NO}_x$  generation.

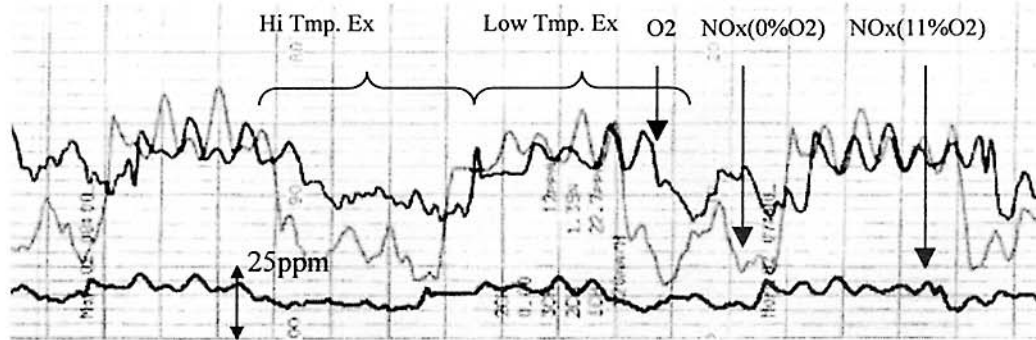


Fig.10 Measurement of NO<sub>x</sub> concentration as a function of Time history

### 3.5 Reduction of delivery period

Our customer has requested us to shorten the delivery period to 9 months. The average period of construction is 1.5 years. It is 2 years when the planning period is included.

In order to reduce this period, the design, the materials, the manufacture, the construction and the test run were reexamined.

#### 1) Concurrent job

The period for designing, arrangement and manufacturing was shortened by means of a concentration of manpower.

#### 2) The new design system using three-dimensional CAD

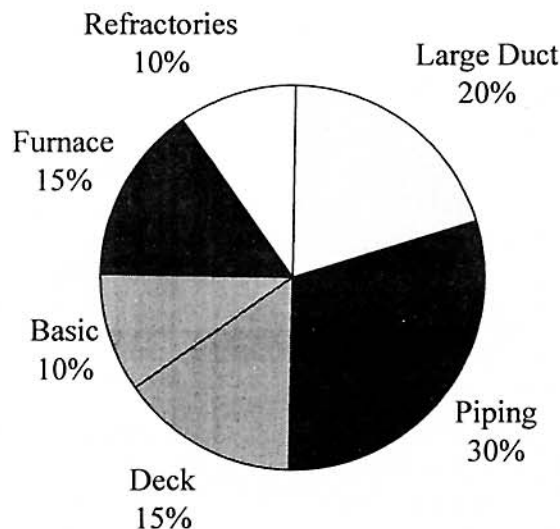


Fig.11 Working time ratio for design

Fig.11 shows a working time ratio for the design. The large duct, various piping, and the check deck occupy 65% of the whole. Conventional planning for a large duct before construction was just a rough design and planning for a small size duct (cooling water, pilot burner drain) started by sketching the piping on-site after construction in order to shorten the meeting time among designers and to even the man-hours.

The three-dimensional CAD can help us to consider the piping system in detail and give the common information of the piping system to designers. It has shortened the time for designing and for the delivery of drawings. A Small size duct is pre-



fabricated in our factory instead of on-site manufacturing. The CAD enabled us to check the gap between the pipe and electronics equipment (rack, wire-duct).

### 3) Rebuilding and test run process

Following points were put into practice.

- (1) Day-and-night 2 shift operations.
- (2) By setting up the temporary stage for materials, the mutual interference of construction work and customer operations was minimized.
- (3) A temporary monorail carrier efficiently carries machine equipment and construction materials.
- (4) The amount of on-site work was decreased by changing from on-site manufacturing small diameter pipes to prefabrication in the factory.

Fig. 12 shows the delivery time was shortened by 9 months after the above countermeasures in comparison with the conventional method. Our customer estimated that the shortened delivery period by 9 months produced about 27M Euro profit. (profit ¥3000 (25 Euro)/ton Capacity 200ton/h Operating time 20h/day x 270days)

However the construction cost was increased about 1.5 times compared with the conventional ways, so the total cost for the furnace builder went up.

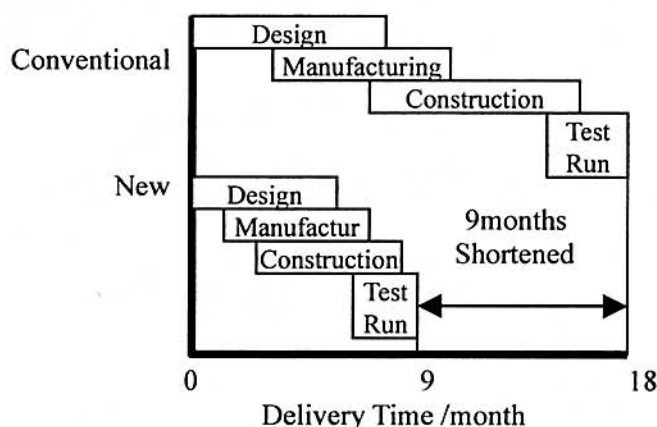


Fig.12 Delivery period for construction

## 4. Conclusion

After applying the highly preheated air combustion to a real furnace, the operation data and the analysis clarified the following points:

- (1) The estimated overall heat transfer coefficient of highly preheated air combustion was 0.95.
- (2) The deviation of temperature distribution was almost flat in the furnace width.
- (3) We confirmed the expansion of the flame and the mixing effect of the exhaust gas by making a high injection velocity of fuel and preheated air.
- (4) The concentration of exhausted  $\text{NO}_x$  was reduced to 20ppm on average as a result of the combustion with low oxygen concentration (11%  $\text{O}_2$ ).
- (5) The indirect heating from constructions inside the furnace made skid mark under 10 °C.
- (6) The period from the design to their delivery was completed in 9 months after being shortened by 9 months.

### **Acknowledgments**

The authors of the present paper are thankful to the NKK Corporation. for its support. We express our hope that our cooperation with the NKK Corporation will be even more successful.